Influence of interfacial defects on the impact toughness of solid state diffusion bonded Ti-6Al-4V alloy based multilayer composites

C.M. Cepeda-Jiménez[1], F. Carreño[1], O.A. Ruano[1], A. A. Sarkeeva[2], A.A. Kruglov[2], R.Ya. Lutfullin[2]

[1]Department of Physical Metallurgy, CENIM, CSIC, Av. Gregorio del Amo 8, 28040 Madrid, Spain

[2]Institute for Metals Superplasticity Problems, 39 Khalturina St., Ufa 450001, Russia

Abstract

Microstructure and mechanical properties, with emphasis in impact toughness behaviour, of two multilayer composites have been investigated. The multilayer materials are constituted by thirteen layers of high strength Ti-6Al-4V alloy. Stacked layers have been successfully joined by diffusion bonding considering two processing temperatures, 750 and 900ºC. The proportion of α/β phase in the microstructure during diffusion bonding process determines the presence of pores at the interface, and therefore the mechanical properties of the composite material. Higher bcc β phase proportion during diffusion bonding process at the highest temperature of 900 ºC leads to high bonding degree, without noticeable toughness increase of the multilayer composite. In contrast, higher proportion of harder hcp α phase at 750ºC makes difficult the healing of interfacial pores, decreasing interfacial toughness and leading to a toughness value of the multilayer composite seven times higher than the reported value for the as-received Ti-6Al-4V alloy.

Keywords: B. Ti-6Al-4V alloy; B. Multilayer materials; C. Diffusion bonding; D. Delamination; D. Interfacial toughness; D. Damage tolerance

*Corresponding author. Tel.: +34 91 5538900; fax: +34 91 5347425.
E-mail address: cm.cepeda@cenim.csic.es (C.M. Cepeda-Jiménez)

1. Introduction

Ti–6Al–4V alloy is well known for two properties: high specific strength and excellent corrosion resistance. In addition, the much higher melting temperature of titanium as compared to aluminium, main competitor in light weight structural applications, gives titanium a definite advantage at temperatures above 150ºC [1,2].

An emerging application for titanium alloys is armour, mainly, but not exclusively, for military vehicles [1]. For this application, an optimized combination of strength and toughness is desirable.

Multilayer composites are being intensively studied for a number of potential applications: electronic devices, structural components, armour, etc. [3-6]. In particular, from a mechanical point of view, multilayer materials are able to reach an outstanding result of strength and toughness simultaneously [7-12].

Toughening mechanisms in materials can be broadly divided into two categories, intrinsic and extrinsic. Intrinsic toughening implies inherent resistance of the microstructure to crack growth (grain size effects, precipitates, particle spacing, etc). Extrinsic toughening is induced by the rest of mechanisms that reduce local stress intensity at the crack tip, for instance delamination at interfaces [13]. Delaminations in layers ahead of the crack tip result in a reduction and redistribution of local stress. Further crack growth requires re-nucleation, i.e. a significant amount of energy absorption, resulting in an increase in toughness [14].

Diffusion bonding is an attractive processing method to obtain multilayer materials [15-17]. This process is dependent on various parameters, in particular, time, applied pressure, and bonding temperature to promote microscopic atomic movement to ensure complete metallurgical bond [18].

On the other hand, titanium materials are primarily corrosion resistant since they are able to form a dense oxide layer after a short period of time in air. This protective layer has tendency to diffuse into the material at high temperatures. This “self-cleaning” characteristic of titanium, together with good solid-state diffusion, results advisable for processing multilayer materials by diffusion bonding [19].

Interfacial properties have been shown to greatly affect the mechanical behaviour of composite multilayers laminates [20-22], because interfaces are numerous and susceptible to decohesion and sliding [23]. Interface decohesion is most likely when the interface toughness is relatively low. It is known that the quality of a diffusion bonded interface depends on the presence or absence of micropores and remnants of oxide particles [24]. Thus, the presence of these defects formed during processing as a consequence of different processing conditions can affect mechanical properties of interfaces favouring delamination as a principal mechanism of crack arresting in multilayer materials, and thus may improve the extrinsic toughening.

Therefore, the aim of this paper is to study the influence of the processing temperature on microstructure and defects formation in the bonding zone, and to correlate it with damage tolerance and interfacial shear mechanical properties of two diffusion bonded multilayer composites obtained. The phase diagram for the Ti-6Al-4V alloy should help clarify phase changes that take place at the processing temperatures considered and thus, microstructural features that affect strongly the fracture behaviour.

2. Experimental procedure

2.1. Materials and processing

Thirteen Ti-6Al-4V sheets of ~0.86 ± 0.02 mm in thickness were stacked, making up a bundle of ~10.9 mm in thickness, ~105 mm in width and ~220 mm in length. The as-received sheets were provided by VSMPO, Verhnyaya Salda, Russia. With the objective of minimizing anisotropy in mechanical properties of this hcp α-based Ti alloy, sheets were stacked varying alternatively the as-received rolling direction 90 degrees. The composition (in weight per cent) of the Ti-6Al-4V alloy was 6.27 Al, 4.22 V, 0.18 Fe, less than 0.001 H, less than 0.01 N, 0.2 O and balance titanium.

The multilayers materials were manufactured by diffusion bonding in a vacuum furnace under argon pressure using a flexible membrane. Processing was performed using two different regimes to control the presence of micropores in interfaces: 1) 750 ºC during 2 h and 3 MPa; and 2) 900 ºC during 2 h and 3 MPa. After processing, the multilayer composites were cooled in a vacuum furnace to room temperature, and additional thermal treatment was not performed. The average thickness of the titanium layers in the multilayer composites processed at 750 and 900ºC was ~860±8 μm and ~870±17 μm, respectively.

2.2. Microstructural determination

In this work, to avoid confusion, a different notation for the sample reference system is used instead of the traditional RD, TD and ND directions. The reference system is shown in Fig. 1a and defined as follows: the interface direction is designated by ID, normal direction to the multilayer composite remains designated by ND as well as transversal directions remains named TD. As, initially, sheets were stacked alternating the as-received rolling direction by 90 degrees, the microstructure at bond interfaces was analyzed in one of the equivalent transversal sections (Fig. 1a). Thus, the plane to be microstructurally characterized always contains ID and ND directions.

Optical and scanning electron microscopy (SEM) using a JXA-6400 instrument were considered. The linear intercept method was used to estimate grain size. At least 300 grains were analyzed to measure grain size. Metallographic preparation involved methods of standard surface preparation. Optical metallography was performed using an etchant agent consisting in 50 ml H_2O + 25 ml HNO_3 +5 ml HF during 10-20 s.

2.3. Mechanical properties

2.3.1. Charpy test

Two mm U-notched Charpy type testing samples were machined with 10x10x55 mm^3 dimensions from diffusion bonded multilayer materials processed at two different temperatures. Crack propagation in the multilayer composites has been studied in two orientations, as shown schematically in Fig. 1: c) crack arrester and d) divider orientation. In crack arrester orientation (Fig. 1c), the initial notch/crack tip ends within an individual layer of the test sample such that the crack front “sees” each layer interface sequentially during loading. In crack divider orientation (Fig. 1d), the initial notch/crack tip intersects all test

sample layers such that the crack front "sees" all the layer interfaces simultaneously [11]. Three samples of each material were tested.

2.3.2. Shear test

To characterize precisely mechanical properties of interfaces, shear tests along them have been performed. Interface mechanical properties were measured by shear test in a *Servosis* universal test machine (cross-head rate=0.005 mm/s) using samples of approximate dimensions 10x10x3 mm^3. Shear test was performed by clamping the sample between two metal supports (Figure 1b). The interface to be tested is located just outside the tool border and parallel to the load direction. Then, a square punch at a given gap distance is used to apply the shear load until interface failure. Shear stress, τ, and shear strain, γ, are given by the expressions [25]:

$$\tau = p/ae \qquad \gamma = tan(\alpha) = d/l_{gap} \qquad (1)$$

where a is sample initial width, e is initial thickness, p is force applied on the sample, d is midspan displacement, α is shear angle and l_{gap} is distance between the supports and the mobile punch, corresponding to 0.35 mm in this study. Therefore, the chosen cross-head rate is equivalent to a shear strain rate about 1.4 10^{-2} s^{-1}.

According to the sample reference system defined in Fig.1a and considering that the transversal sections in the multilayer material are equivalent, the plane to be sheared during the shear test always contains ID and TD directions, as shown in Fig.1b.

Once shear tests were carried out, fracture surfaces were analyzed using SEM to asses more precisely the type of failure of the bonded layers.

3. Results

3.1. Microstructure

Fig. 2a shows the microstructure of the as-received Ti–6Al–4V in the rolling plane, which consists of equiaxed α grains ~3 μm in size surrounded by the equilibrium volume fraction of β phase along grain boundaries of α grains. Figure 2b shows the phase diagram for the Ti-6Al-4V alloy in the α+β region [26] of interest for processing of multilayer materials in the present work. As mentioned, two temperatures during diffusion bonding process have been considered, 750 and 900ºC. Between 750 and 900ºC the proportion of β phase varies from about 10% to 50% [27]. The influence of different phase proportion during processing at different temperature on microstructure and interfacial mechanical properties will be analyzed in the discussion.

Fig. 3 shows optical (a and c) and secondary electron (b and d) micrographs corresponding to cross-sections of the two multilayer composites processed in this work. Fig. 3a and b correspond to the material processed at 900ºC, and Fig. 3c and d correspond to that

processed at 750ºC. Micrographs were taken close to interfaces and these are located in the middle of the images.

After diffusion bonding process, the microstructure of the Ti-6Al-4V alloy is characterized by equiaxed grains, with sizes 5.4 ± 1.8 and 2.9 ± 1.2 μm for the multilayer composites processed at 900 and 750 ºC, respectively.

The interface between two layers illustrates retention of equiaxed α microstructure and presence of pores or voids. However, the pores fraction is considerably higher for the multilayer material processed at lower temperature (Fig.3c and d) than that for the processed at 900 ºC (Fig.3a and b). Long pores having lengths up to 60 μm, continuously distributed along interfaces, were observed in the material processed at 750ºC.

The quality of solid state bonding has been evaluated by the relative length of defects (L_p) (micropores) according to the relation:

$$L_p=(L_{pi}/L_0) \times 100\ (\%) \qquad (2)$$

where L_{pi} is the total length of pores along the interface and L_o is the gauge length of the analyzed interface. The relative length of pores (L_p) was ~1% for the multilayer composite processed at 900ºC, while L_p for the material diffusion bonded at 750ºC was ~32%.

3.2. Mechanical properties

3.2.1. Charpy test

The impact toughness value reported [28] for monolithic Ti-6Al-4V alloy, determined using as in the current work samples with 10x10x55 mm^3 dimensions and 2mm U-notch, was 450 kJ/m^2. The two multilayer materials possess higher impact energy in crack arrester orientation than the reported value for monolithic Ti-6Al-4V alloy, being ~570 kJ/m^2 and >3200 kJ/m^2 for the laminate processed at 900 and 750ºC, respectively. In contrast, only the multilayer composite without pores in the interfaces showed higher damage tolerance in divider orientation (~660 kJ/m^2). It is worth noting the high impact toughness value of the multilayer material containing pores in interfaces in crack arrester orientation (>3200 kJ/m^2), which is more than seven times higher than that for monolithic material. Furthermore, due to its high impact toughness, this sample was not broken and stopped the pendulum. This difference in behaviour between the two multilayer composites is related to higher volume fraction of pores in interfaces of the multilayer material processed at 750ºC, as shown in Fig.3, which decreases the bonded area and favours a possible delamination. In contrast, a lower absorbed energy value (~570 kJ/m^2) in the high temperature processed material (without pores) in crack arrester orientation can be attributed to a stronger interlayer bond. Likewise, the impact toughness increase observed in crack divider orientation for the composite without pores in interfaces (~660 kJ/m^2), in comparison with that for the composite with pores (~420 kJ/m^2), also can be attributed to this high bonding degree achieved in the first one. It has been reported [29] that layer plasticity in laminated composites can be

enhanced by introducing tougher interfaces, which can strongly constrain and delay the failure development or local necking of individual layers when the laminate is tensile tested and, as in the current work in divider orientation, all layers are simultaneously tested. Thus, this plasticity increase of individual layers enhances material damage tolerance in this orientation (crack divider).

The multilayer composite processed at the highest temperature showed typical fracture behaviour of monolithic materials, i.e, crack propagates without interruption sequentially in adjoining layers. Therefore, the impact toughness increase for the multilayer composite must be attributed to intrinsic contribution of recovery and elimination of internal stresses during processing at high temperature.

However, macrographs of Charpy tested samples for the multilayer material processed at 750ºC show different fracture behaviour (Fig. 4). Fig.4a shows the macrograph corresponding to the Charpy sample tested in crack arrester orientation, where long delaminations with extensive plastic deformation of titanium layers can be observed. Delaminations enlarge the absorbed energy because it makes difficult crack propagation in the next layer which must deform plastically until a new dominant crack is nucleated. Thus, the longer the extent of debonding at layers interface, the larger is impact toughness. The macrograph corresponding to the composite with pores in crack divider orientation (Fig. 4b) also shows evidence of interface debonding together with some plastic tearing of Ti-6Al-4V layers.

3.2.2. Shear tests

To characterize precisely mechanical properties of interfaces, which are responsible of the damage tolerance increase, shear tests have been performed. Figure 5a shows a representation of shear stress versus shear strain obtained from shear tests on interfaces for the two Ti-6Al-4V multilayer composites processed at different temperatures. For comparison, shear curves of a Ti-6Al-4V alloy that was tested simulating monolithic configuration have been also included. For this purpose, the multilayer materials were rotated 90 degrees, as shown in Fig. 5b, such that all interfaces are tested simultaneously during shear test, and thus, their effect is nearly negligible. Accordingly, the material behaves as monolithic. Also, Table 1 includes values of mechanical properties extracted from various shear curves of different materials, and average values for each material configuration. Shear toughness of interfaces was measured as the area under load-displacement curves. Several samples for every configuration were tested. Hence, the different tested interfaces are labelled by numbers indicating their location in the multilayer material in respect to the outer layer (e.g. s3-i5 means sample 3 and fifth interface from surface).

Firstly, clear differences in elastic modulus are observed between different curves (Fig.5a). This is attributed to an effect of texture by the inherent anisotropy of the α phase of titanium.

The Ti-6Al-4V alloy in monolithic configuration shows values of maximum shear stress between 447 and 552 MPa, and shear strain between 2.04 y 2.97 (Fig. 5a and Table 1). In general, all interfaces of the multilayer materials present lower strength and ductility than those of the monolithic alloy configurations, i.e. lower interfacial toughness.

Regarding the interfaces of the Ti-6Al-4V multilayer composite processed at high temperature and without pores, shear curves show some plastic deformation prior to fracture, and the interfacial toughness is about half than that for the Ti-6Al-4V alloy in monolithic configuration (Table 1). In contrast, the multilayer material tested at 750ºC containing pores in interfaces, shows quite brittle interfaces, with a lower maximum shear stress (455 MPa) than the composite processed at 900ºC, and also lower values of shear deformation to failure ranged between 0.77 and 0.90. The interface toughness for this material is about a quarter that of the monolithic alloy (Table 1), being for some interfaces considerably lower (55-58 kJ/m^2) than the shear toughness for its constituent material (291 kJ/m^2). It can be concluded that the interface toughness decreases when the volume fraction of pores is increased.

Figure 6 shows SEM micrographs at two magnifications of fractured surfaces from shear tests for the monolithic Ti-6Al-4V alloy (Fig.6a and b), and multilayer composites processed at different temperatures (Fig. 6c-f). Fig. 6a and b illustrates a ductile fracture by microvoid coalescence and plastic stretching.

On the other hand, the fractured surfaces of the multilayer composites correspond to zones where maximum deformation was reached and interfacial failure occurred. The SEM micrographs of the composite processed at 900ºC (Fig. 6c and d) shows a very ductile fracture surface with a similar appearance than the failure for the monolithic alloy, indicating high bonding degree according to the nearly perfect interface observed previously (Fig. 3a and b). However, this sample shows a mixture failure, being initially ductile in the Ti-6Al-4V bulk, but after reaching the maximum shear stress, the failure is produced along the interface between layers in a catastrophic manner (Fig. 5a).

Furthermore, the fractured surfaces corresponding to the composite processed at 750ºC (Fig.6e-f) present a less ductile behaviour. The surface topography of the failed surface reveals perfectly bonded areas between layers and non-bonded areas due to pores or defects, which are observed in Fig.6e as dark perpendicular lines, indicating the pores distribution in interfaces after diffusion bonding processing. The presence of these non-bonded areas determines the low interfacial toughness, because, as commented, these non-bonded areas facilitate crack nucleation and propagation. This is consistent with delaminations observed under Charpy impact test of the composite with pores that leads to an increase of toughness in crack arrester orientation by an extrinsic crack deflection mechanism. Although these interfaces are less ductile than those of the material processed at high temperature, they present high maximum stress (Table 1), which is an indication of high bond integrity.

4. Discussion

In the present work, two multilayer composite materials based on Ti-6Al-4V alloy have been processed by diffusion bonding at two different temperatures. Diffusion bonded interfaces with high integrity, i.e. high strength and adequate ductility, have been obtained at relatively low temperature of 750ºC, delivering a multilayer material with outstanding impact toughness in crack arrester orientation. This is the most interesting testing orientation from a technological point of view because it is the natural configuration for a possible application to enhance damage tolerance, for example in the fuselage in an airplane.

On the other hand, it is worth noting that material toughness in crack arrester will be higher if the interface toughness is relatively low, as observed for the multilayer composite with pores in interfaces.

A comparison of the microstructure of the multilayer material processed at 750 ºC (Fig. 3c and d) respect to that processed at 900 ºC (Fig. 3a and b) reveals a finer grain size and lower bonding degree with ~32% of micropores along interfaces for the material processed at low temperature. In contrast, as seen in Fig. 3, the fraction of micropores is nearly negligible at the highest diffusion bonding temperature, 900 ºC (~1%). Furthermore, at this temperature, the Ti-6Al-4V alloy shows only limited grain growth (~5.4 μm) in comparison with the as-received alloy (~3 μm) (Fig. 2a). As commented previously, the increase in processing temperature up to 900ºC emerges the presence of the high-temperature β phase (Fig. 2b). The presence of this β phase at 900ºC accelerates grain growth, as evidenced in Fig. 3b after $\beta \rightarrow \alpha$ transformation after cooling to room temperature.

Although grain size influences mechanical behaviour of Ti alloys, the small difference in grain sizes observed in these multilayer composites investigated is not considered determinant for the purpose of this study.

In addition, during the diffusion bonding process and "healing" of pores with increase of temperature, most of grains remain equiaxed. This is difficult to be explained only by diffusion of atoms. In a previous work [30], it was demonstrated by annealing treatments that the relative pore length decreases very slightly when the formation of the solid state joint is determined only by diffusion processes. Furthermore, this phenomenon was observed in microcrystalline titanium alloys, as in the current work, where the role of grain boundary diffusion is important. Obtained data testified that deformation plays the prevailing role in the process of solid state joint formation, and pore disappearance process was already observed at ε~5%. By direct local observation of the interface formation, this study [30] confirmed that pores healing was performed by shift and/or rotation of grains relative to each other in the vicinity of bonded interfaces due to grain boundary sliding (GBS). It is our contention that GBS can be significantly activated in the current work, since the local deformation in the field of the bonded area due to the initial roughness may be more than 5%. Furthermore, it also has been widely reported [31-33] that the optimum temperature for superplastic deformation of conventional Ti-6Al-4V alloy with ~ 10μm grain size is 900ºC. Thus, it is likely that during

diffusion bonding three simultaneous mechanisms would be acting: grain boundary sliding, grain rotation and grain boundary diffusion.

On the other hand, diffusion bonding is performed typically at temperatures in the (α+β) phase field. The existence of two different crystal structures and the corresponding allotropic transformation temperature is of central importance, since they are the basis for the large variety of properties achieved by titanium alloys [1].

As mentioned and according to the phase diagram for Ti-6Al-4V alloy (Fig. 2b), between 750 and 900ºC the proportion of β phase varies from about 10% to 50% [27]. Thus, at the low processing temperature of 750ºC, the proportion of β phase is low and the harder α phase dominates the deformation behaviour. Generally, the number of independent slip systems is only 4 for the polycrystalline hcp α titanium structure while it is at least 12 for the bcc lattice, justifying the limited plastic deformability of the hcp α titanium compared to the bcc β titanium [34]. For α titanium the main slip directions are the three close-packed directions of the type <1120>, and the slip planes containing these slip directions are the (0002) plane, the three {1010} planes, and the six {1011} planes. Among these three different types of slip planes together with the possible slip directions there are a total of 12 slip systems. However, these can be reduced to nominally 4 independent slip systems, because although prismatic and basal planes have three slip systems each, only two are independent of each other, resulting in only four independent slip systems. In addition slip on pyramidal planes does not increase the number further since this glide is composed of a prism and a basal component and therefore cannot be considered an independent slip system. Therefore, assuming the von Mises criterion is correct, which requires at least five independent slip systems for a homogenous plastic deformation of polycrystals, the operation of one of the slip systems with a so-called non-basal Burgers vector needs to be activated.

Accordingly, at 750ºC grain boundaries and triple-point β phase would deform only if the α phase deforms, although the β phase could facilitate a limited amount of sliding between α grains. In addition, the diffusion coefficient of α titanium is orders of magnitude smaller than that of bcc β titanium because of the densely packed atoms in hcp α titanium. This limited plastic deformability and diffusion of the hcp α phase explains the high volume fraction of pores in interfaces for the multilayer composite processed at 750ºC, and the difficulty for healing them during processing.

However, the high volume fraction of pores in their interfaces favours lower interfacial toughness and activation of extrinsic toughening mechanisms such as delamination and crack renucleation which, as commented previously, improve the multilayer material toughness in crack arrester orientation. From interfacial toughness values obtained by shear tests (Fig. 5) and included in Table 1 it can be observed that the interfacial toughness for the material processed at the lowest temperature is about a quarter than that for the monolithic configuration. Previous results [35] predicted that crack goes through the interface if the

interface toughness exceeds about 1/4 of the material toughness across the interface. Therefore, and according to this relation, the composite containing high amount of pores in interfaces presents interfaces prone to delamination. In addition, after every delamination as observed in Fig.4a, Ti-6Al-4V layers must be hardened and plastic strained until a new crack will be renucleated. Thus the extra work of deformation contributes to the overall toughness, which is more than seven times higher than the reported value [28] for monolithic material.

In contrast, above 875ºC the fraction of β phase increases rapidly with increasing temperature up to the β-transus (990-1010ºC). Thus, at the highest processing temperature of 900 ºC, large amount of β phase is present and properties of the Ti-6Al-4V alloy are dominated by the softer β phase. This phase facilitates rotation, translation and rearrangement of α grains, being the properties of β phase more apparent [27], justifying the high bonding degree observed at high processing temperature (Fig.3a and b).

Therefore, at high processing temperature when GBS and high diffusivity degree is possible, pores and defects in interfaces are progressively healed, and this causes increase of interfacial toughness, as determined by shear tests (Fig. 5 and Table 1). Thus, the lower relative increase in absorbed energy during Charpy test for the multilayer composite processed at 900ºC without pores in interfaces in crack arrester orientation (~570 kJ/m^2), respect to that processed at 750ºC (>3200 kJ/m^2), is attributed to tougher interlayer bond, not being prone to delaminate. This is clearly corroborated by the largest area under the shear test curves for the material processed at 900ºC (Fig. 5), and the presence of a ductile fracture (Fig. 6c,d), with similar appearance to that of the monolithic Ti-6Al-4V alloy (Fig. 6a,b) shear tested under similar test conditions.

In summary, the volume fraction of pores as a function of processing temperature and proportion of α/β phases during diffusion bonding affects the interface toughness, its fracture mechanism, and thus, the multilayer material toughness.

5. Conclusions

Two multilayer composites based on Ti-6Al-4V alloy have been obtained by diffusion bonding at two different temperatures (750 and 900ºC), conducted to improve impact toughness of this alloy. The major conclusions of the study are:

1. Optimised interface toughness can be obtained by temperature processing control, taking into account the proportion of α/β phase in the microstructure during diffusion bonding.

2. Higher β phase proportion during diffusion bonding process at the highest temperature of 900ºC favours higher diffusivity, grain rotation and grain boundary sliding, leading to high bonding degree with almost imperceptible interfaces. Accordingly, the multilayer material processed at 900ºC resembles a monolithic material, without noticeable toughness increase.

3. The presence of harder hcp α phase during processing at the lowest temperature of 750ºC makes difficult the contact between layers, avoiding healing of interfacial pores. Therefore, the multilayer composite processed at 750ºC presents ~32% relative length of pores in interfaces, which decreases interfacial toughness. Accordingly, the lower the interfacial toughness, the higher the overall material toughness in crack arrester orientation, which is more than seven times higher than the reported value for the as-received Ti-6Al-4V alloy.

4. The Ti-6Al-4V multilayer composite processed at 750ºC offers an excellent combination of specific strength and toughness for possible structural applications.

Acknowledgements

Financial support from MICINN (Project MAT2009-14452) is gratefully acknowledged.

References

1. G. Lutjering, J.C. Williams, Titanium, second ed., Springer-Verlag Berlin Heidelberg, 2003.
2. L. He, A. Dehghan-Manshadi, R.J. Dippenaar, Mater. Sci. Eng. A 549 (2012) 163-167.
3. B.A. Movchan, F.D. Lemkey, Mater. Sci. Eng. A 224 (1997) 136-145.
4. T. Li, F. Grignon, D.J. Benson, K.S. Vecchio, E.A. Olevsky, F. Jiang, A. Rohatgi, R.B. Schwarz, M.A. Meyers, Mater. Sci. Eng. A 374 (2004) 10-26.
5. B.C. Kang, H.Y. Kim, O.Y. Kwon, S.H. Hong, Scripta Mater. 57 (2007) 703-706.
6. J. Han, C. Liao, T. Jiang, C. Spanheimer, G. Haindl, G. Fu, V. Krishnakumar, K. Zhao, A. Klein,W. Jaegermann, J. Alloys. Compd, 509 (2011) 5285-5289.
7. S. Bueno, C. Baudín, Key Eng. Mater. 333 (2007) 17-26.
8. T.M. Osman, P.M. Singh, J.J. Lewandowski, Scripta Metall. Mater. 31 (1994) 607-612.
9. D.R. Lesuer, C.K. Syn, O.D. Sherby, J. Wadsworth, J.J. Lewandowski, W.H. Jr. Hunt, Int. Mater. Rev. 41 (1996) 169-197.
10. M. Pozuelo, F. Carreño, C.M. Cepeda-Jiménez, O.A. Ruano, Metall. Mater. Trans. A 39 (2008) 666-671.
11. C.M. Cepeda-Jiménez, M. Pozuelo, J.M. García-Infanta, O.A. Ruano, F. Carreño, Metall. Mater. Trans. A 40 (2009) 69-79.
12. T. Sinmazçelik, E. Avcu, M.O. Bora, O. Çoban, Mater. Design 32 (2011) 3671-3685.
13. A. Rohatgi, D.J. Harach, K.S. Vecchio, K.P. Harvey, Acta. Mater. 51 (2003) 2933-2957.
14. C.M. Cepeda-Jiménez, J.M. García-Infanta, M. Pozuelo, O.A. Ruano, F. Carreño, Scripta Mater. 61 (2009) 407-410.
15. A.A. Ganeeva, A.A. Kruglov, R.Y. Lutfullin, Rev. Adv. Mater. Sci. 25 (2010) 136-141.
16. H.-S. Lee, J.-H. Yoon, C.H. Park, Y.G. Ko, D.H. Shin, C.S. Lee, J. Mater. Process. Technol. 187-188 (2007) 526-529.

17. L.I. Duarte, F. Viana, A.S. Ramos, M.T. Vieira, C. Leinenbach, U.E. Klotz, M.F. Vieira, J. Alloys Compd. 536S (2012) S424-427.
18. G. He, H. Liu, Q. Tan, J. Ni, J. Alloys Compd. 509 (2011) 7324-7329.
19. W. Beck, Superplastic forming and diffusion bonding of titanium and titanium alloys, in: C. Leyens, M. Peters (Eds.), Titanium and titanium alloys Wiley-VCH, Weinheim, Germany, 2003, pp.278.
20. J. Zhang, J.J. Lewandowski, J. Mater. Sci. 29 (1994) 4022-4026.
21. S. Nambu, M. Michiuchi, J. Inoue, T. Koseki, Compos. Sci. Technol. 69 (2009) 1936-1941.
22. S. Sam, S. Kundu, S. Chatterjee, Mater. Design 40 (2012) 237-244.
23. A.G. Evans, J.W. Hutchinson, Acta Metall. Mater. 43 (1995) 2507-2530.
24. R.Y. Lutfullin, M.K. Mukhametrakhimov, Met. Sci. Heat Treat. 48 (2006) 54-56.
25. G.E. Dieter, Mechanical Metallurgy, SI Metric, UK, 1988, pp.12-15.
26. B.K. Kad, S.E. Schoenfeld, M.S. Burkins, Mater. Sci. Eng. A 322 (2002) 241-251.
27. M.L. Meier, D.R. Lesuer, A.K. Mukherjee, Mater. Sci. Eng. A 136 (1991) 71-78.
28. S. Zherebtsov, E. Kudryavtsev, S. Kostjuchenko, S. Malysheva, G. Salishchev, Mater. Sci. Eng. A 536 (2012) 190-196.
29. H.S. Liu, B. Zhang, G.P. Zhang, Scripta Mater. 64 (2011) 13-16.
30. O.A. Kaibyshev, R.Y. Lutfullin, V.K. Berdin, Acta Metall. Mater. 42 (1994) 2609-2615.
31. G.A. Salishchev, R.M. Galeyev, O.R. Valiakhmetov, R.V. Safiullin, R.Y. Lutfullin, O.N. Senkov, F.H. Froes, O.A. Kaibyshev, J. Mater. Process. Technol. 116 (2001) 265-268.
32. G. Giuliano, Mater. Design 29 (2008) 1330-1333.
33. V. Sinha, R. Srinivasan, S. Tamirisakandala, D.B. Miracle, Mater. Sci. Eng. A 539 (2012) 7-12.
34. M. Peters, J. Hemptenmacher, J. Kumpfert, C. Leyens, Structure and properties of titanium and titanium alloys, in: C. Leyens, M. Peters (Eds.), Titanium and titanium alloys Wiley-VCH, Weinheim, Germany, 2003, pp.5.
35. J.W. Hutchinson, A short sourse on the integrity of thin films and multilayers, National University of Singapore, Singapore, 1997, pp. 21.

Figure Captions

Figure 1. Schemes of: a) the reference system considered in this work for multilayer composites; b) shear test; and samples for Charpy impact test: c) crack arrester orientation, and d) crack divider orientation.

Figure 2. a) SEM micrograph showing the microstructure of the as-received Ti-6Al-4V alloy, and b) Ti-6Al-4V phase diagram in the $\alpha+\beta$ region of interest for processing of multilayer composites [26].

Figure 3. a) and c) Optical and b) and d) SEM micrographs showing the microstructure close to interfaces. a) and b) correspond to the Ti-6Al-4V multilayer composite processed at 900ºC without pores in interfaces; and c) and d) correspond to the Ti-6Al-4V multilayer composite processed at 750ºC with pores in interfaces.

Figure 4. Macrographs of fractured samples of the Ti-6Al-4V multilayer composite with pores in interfaces from Charpy tests: a) Crack arrester orientation and (b) Crack divider orientation.

Figure 5. a) Stress-strain curves from shear tests conducted on monolithic configurations and different interfaces of composites with and without pores in interfaces. b) Schemes of multilayer composite orientations considered to test interfaces in multilayer materials and Ti-6Al-4V alloy in monolithic configuration. SLD is referred to shear load direction.

Figure 6. SEM micrographs at different magnifications showing interfacial fractured surfaces from shear tests of: a) and b) monolithic Ti-6Al-4V alloy; c) and d) Ti-6Al-4V multilayer composite processed at 900ºC without pores in interfaces; and e) and f) Ti-6Al-4V multilayer composite processed at 750ºC with pores in interfaces.

Table 1. Mechanical properties of the monolithic Ti-6Al-4V alloy and interfaces in the Ti-6Al-4V multilayer composites from shear tests (s=sample; i= interface; τ_{max}= maximum shear strength; $\gamma_{shear\ max.}$= maximum shear strain; A= area under shear load-displacement curve corrected by the tested section).

Material	**Sample**	**τ_{max} (MPa)**	**$\gamma_{shear\ max.}$**	**A (kJ/m^2)**
Monolithic Ti-6Al-4V				
Without pores	s1	447	2.97	392
	s2	515	2.24	290
Average		**481±48**	**2.61±0.52**	**341±72**
With pores	s1	552	2.10	298
	s2	541	2.04	284
Average		**547±8**	**2.07±0.04**	**291±10**
Ti-6Al-4V composite without pores	s1-i3	520	1.41	170
	s1-i5	485	1.25	136
	s2-i2	507	1.33	153
	s2-i4	510	1.32	150
	s3-i2	501	1.40	163
	s3-i5	489	1.30	145
Average		**502±13**	**1.34±0.06**	**152±12**
Ti-6Al-4V composite with pores	s1-i4	400	0.77	55
	s2-i4	469	0.82	71
	s2-i7	479	0.86	77
	s3-i2	490	0.90	83
	s3-i5	461	0.84	71
	s3-i7	448	0.86	70
	s4-i3	465	0.87	75
	s4-i6	428	0.75	58
Average		**455±29**	**0.83±0.05**	**70±9**

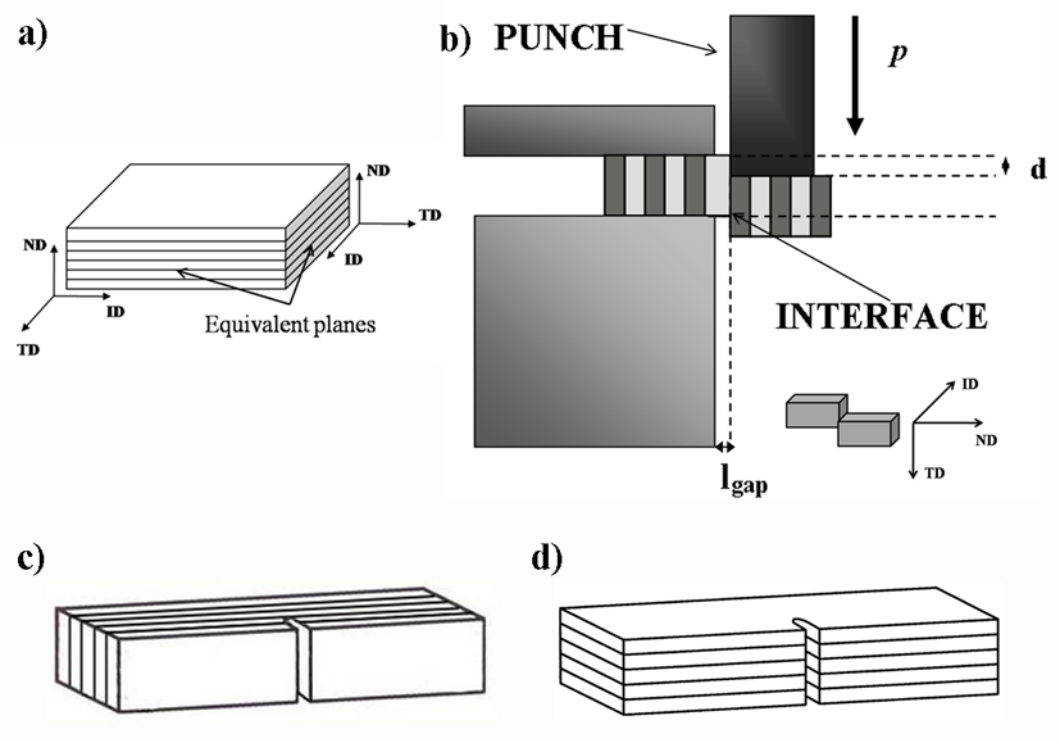

Figure 1. Schemes of: a) the reference system considered in this work for multilayer composites; b) shear test; and samples for Charpy impact test: c) crack arrester orientation, and d) crack divider orientation.

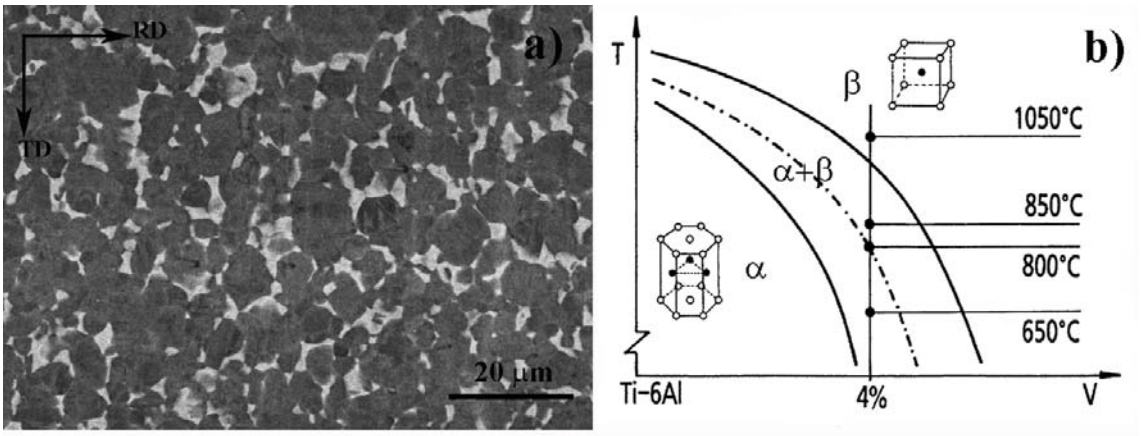

Figure 2. a) SEM micrograph showing the microstructure of the as-received Ti-6Al-4V alloy, and b) Ti-6Al-4V phase diagram in the α+β region of interest for processing of multilayer composites [26].

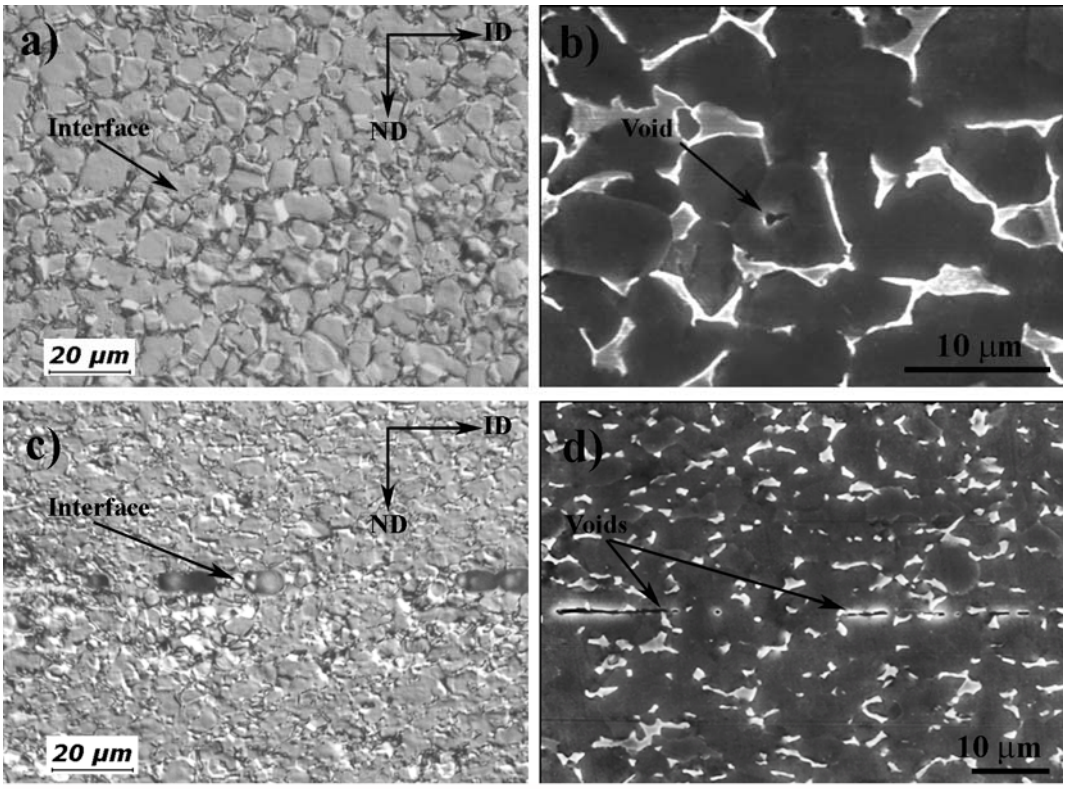

Figure 3. a) and c) Optical and b) and d) SEM micrographs showing the microstructure close to interfaces. a) and b) correspond to the Ti-6Al-4V multilayer composite processed at 900ºC without pores in interfaces; and c) and d) correspond to the Ti-6Al-4V multilayer composite processed at 750ºC with pores in interfaces.

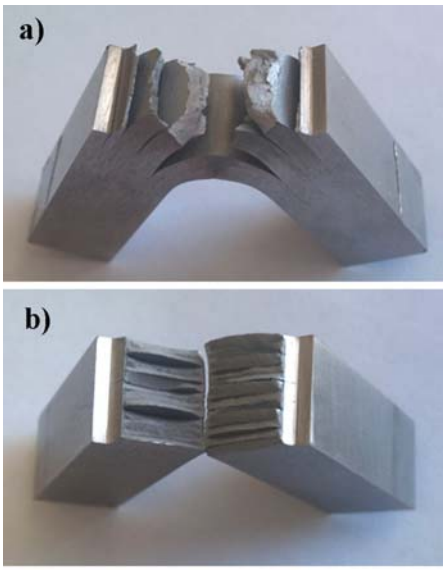

Figure 4. Macrographs of fractured samples of the Ti-6Al-4V multilayer composite with pores in interfaces from Charpy tests: a) Crack arrester orientation and (b) Crack divider orientation.

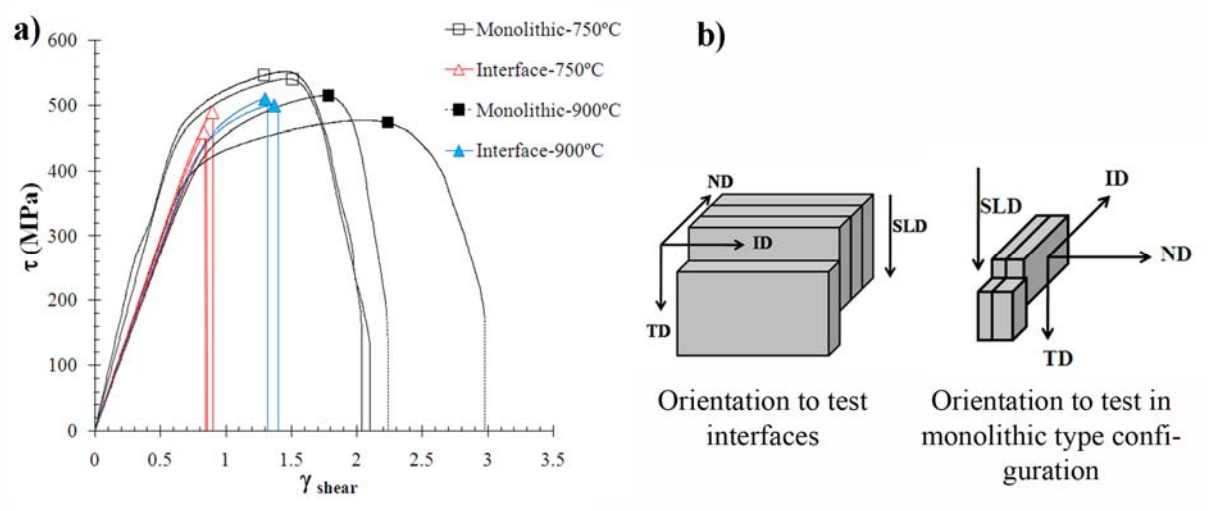

Figure 5. a) Stress-strain curves from shear tests conducted on monolithic configurations and different interfaces of composites with and without pores in interfaces. b) Schemes of multilayer composite orientations considered to test interfaces in multilayer materials and Ti-6Al-4V alloy in monolithic configuration. SLD is referred to shear load direction.

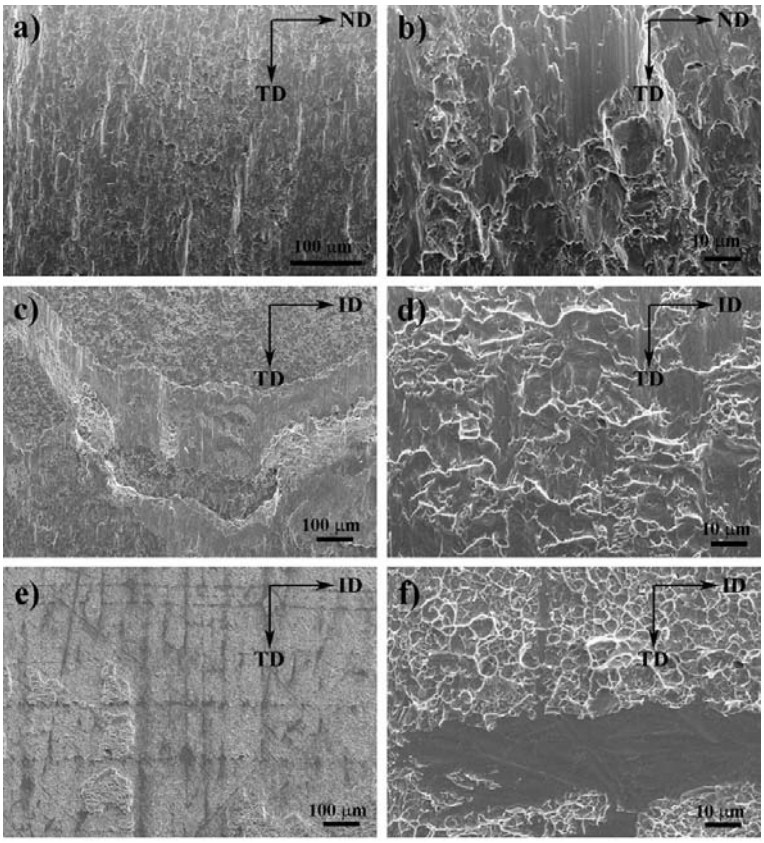

Figure 6. SEM micrographs at different magnifications showing interfacial fractured surfaces from shear tests of: a) and b) monolithic Ti-6Al-4V alloy; c) and d) Ti-6Al-4V multilayer composite processed at 900ºC without pores in interfaces; and e) and f) Ti-6Al-4V multilayer composite processed at 750ºC with pores in interfaces.